Morphologies in Ternary Polymer Blends after Spin-Coating

Stefan Walheim, Marcus Ramstein, and Ullrich Steiner*

Fakultät für Physik, Universität Konstanz, D-78457 Konstanz, Germany

Received October 20, 1998. In Final Form: December 4, 1998

The domain morphology of a polystyrene/poly(methyl methacrylate)/poly(2-vinylpyridine) (PS/PMMA/PVP) polymer blend was studied after spin-coating a film from a common solvent. The strongly incompatible polymer mixture phase-separates during spin-coating. Atomic force microscopy, combined with selective dissolution of the different polymer phases was used to obtain information on the polymer distribution in the film. By changing the relative composition of the mixture, a great variety of different morphologies was observed. The common feature of all observed morphologies is the compatibilizing function of poly(methyl methacrylate), which intercalates between the more incompatible polystyrene and polyvinylpyridine domains to prevent the formation of high-energy interfaces.

Introduction

Multicomponent mixtures of high molecular weight polymers are of considerable commercial interest since their material properties can be controlled by the blending of several constituent components.[1] While the phase behavior of binary blends has extensively been studied,[2−4] less is known about the phase behavior of multicomponent systems.[5−11] In this context, the investigation of three-component systems is particularly attractive, since in many cases, one of the components will act as an interfacial compatibilizer between the other two phases.[12,13] For example, the addition of a copolymer to a binary polymer mixture results in an increase of the fracture toughness of the blend.[14,15] This principle is not limited to the highly specialized case of copolymers. Any agent which reduces the interfacial energy in a binary polymer blend will show a similar effect.

In thin films, the effect of the two bounding interfaces adds an additional complexity to the phase morphologies in ternary blends. Nevertheless, in some special cases, the evolving structures can be understood in simple terms. The spatial organization of the three phases can readily be predicted, if one of the polymer phases (e.g., B) wets the interface of the other two phases (A and C). In this case, the polymer−polymer interactions at the A−C interface are much less favorable compared to the A−B and B−C interfaces (i.e., in a Flory−Huggins model, the interaction parameter χ_{AC} is larger than the sum of χ_{AB} and χ_{BC}). Therefore a B layer intercalates at the A−C interface to reduce the overall free energy. If, in addition, the film surfaces act as neutral boundaries, which do not preferentially adsorb any of the three polymers, a purely two-dimensional phase morphology is expected, with no compositional variation normal to the film boundaries. Such laterally demixed ternary polymer blends in a thin film geometry exhibit a rich variety of morphologies.[6]

For experimental systems, however, the imposition of neutral boundaries poses a problem since chemically different polymers will usually show a different affinity to a given surface. For polar surfaces, this difference will generally be more important due to the large polymer−surface interfacial energies. In the absence of specific interactions, unpolar surfaces feature lower values of the polymer−surface interfacial tensions and thereby also the lower specific adsorption of one of the components. A film sandwiched between two unpolar surfaces is therefore a good experimental realization of the quasi-two-dimensional case described above.

In this article, we describe the phase morphology of a model ternary polymer blend between two unpolar surfaces: a thin film of polystyrene (PS), poly(methyl methacrylate) (PMMA), and poly(2-vinylpyridine) (PVP) spin-cast from a common solvent onto an unpolar substrate.

Experimental Section

Materials. In this work polystyrene, poly(methyl methacrylate), and polyvinylpyridine were purchased from Polymer Standards Service and used as obtained. Their characteristics are listed in Table 1. The polymers were dissolved in analytic grade tetrahydrofuran (THF) (stabilized with 250 mg/L 2.6-di-*tert*-butyl-4-methylphenol). All concentrations and volume fractions are given in weight percent. Polymer films were prepared by spin-coating from PS−PMMA−PVP solutions (typically 3% polymer). The film thickness was controlled by varying the rotation speed (typically 7000 rpm). The average film thickness ranged from 100 to 120 nm. Macroscopic examination of the

* To whom correspondence should be addressed. Tel: +49-7531-883824. Fax: +49-7531-883072. E-mail: ulli.steiner@uni-konstanz.de.

(1) Utracki, L. A. *Polymer Blends and Alloys* Hanser: New York, 1989.
(2) Gunton, J. D.; San Miguel, M.; Sahni, P. S. In *Phase Transitions and Critical Phenomena*; Domb, C., Lebovitz, J. L., Eds.; Academic Press: New York, 1983; Vol. 5.
(3) Binder, K. In *Materials Science and Technology*; Haasen, P., Ed.; VCH-Verlag: Weinheim, 1990; Vol 5.
(4) Krausch, G. *Mater. Sci. Eng.* **1995**, *R14*, 1−94.
(5) Hobbs, S. Y.; Dekkers, M. E. J.; Watkins, V. H. *Polymer* **1988**, *29*, 1598−1602.
(6) Nauman, E. B.; He, D. Q. *Polymer* **1994**, *35*, 2243−2255.
(7) Yeung, C.; Desai, R. C.; Noolandi, J. *Macromolecules* **1994**, *27*, 55−62.
(8) Huang, C.; Olvera de la Cruz, M.; Swift, B. W. *Macromolecules* **1995**, *28*, 7996−8005.
(9) Faldi, A.; Genzer, J.; Composto, R. J.; Dozier, W. D. *Phys. Rev. Lett.* **1995**, *74*, 3388−3391.
(10) Guo, H. F.; Packirisamy, S.; Gvozdic, N. V.; Meier, D. J. *Polymer* **1997**, *38*, 785−794.
(11) Genzer, J.; Composto, R. J. *Macromolecules* **1998**, *31*, 870−878.
(12) Israels, R.; et al. *J. Chem. Phys.* **1995**, *102*, 8149.
(13) Gersappe, D.; Irvine, D.; Balazs, A. C.; Liu, Y.; Sokolov, J.; Rafailovich, M.; Schwarz, S.; Pfeiffer, D. G. *Science* **1994**, *265*, 1072−1074.
(14) Brown, H. *Annu. Rev. Mater. Sci.* **1991**, *21*, 463.
(15) Dai, C.-A.; Dair, B. J.; Dai, K. H.; Ober, C. K.; Kramer, E. J.; Hui, C.-Y.; Jelinski, L. W. *Phys. Rev. Lett.* **1994**, *73*, 2472.

10.1021/la981467e CCC: $18.00
Published on Web 00/00/0000 PAGE EST: 8.7

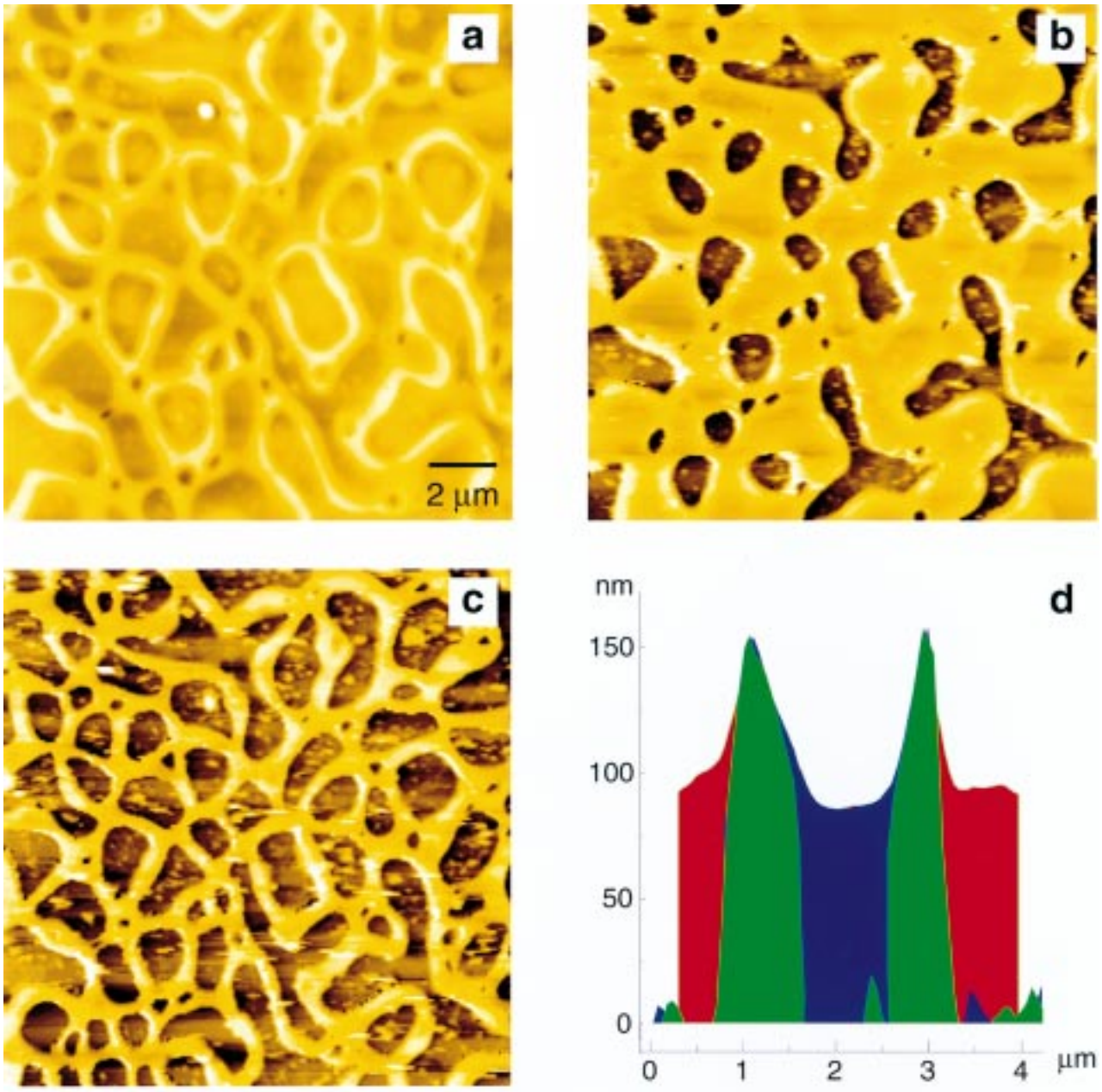

Figure 1. AFM images of a PS/PMMA/PVP film (1:1:1) cast from THF onto a SAM-covered surface: (a) as cast; (b) after immersion in ethanol to remove PVP; (c) after removal of PS by dissolution in cyclohexane. The PMMA phase forms a quasi-two-dimensional network which separates the PS and PVP domains. In (d) cross sections from (a−c) were superimposed to show the polymer composition in the film (PS, blue; PMMA, green; PVP, red).

Table 1. Molecular Characteristics[a]

polymer	mol wt	polydispersity index
PS	94.9k	1.06
PMMA	126k	1.04
PVP	115k	1.03

[a] All materials were bought from Polymer Standards Service, Mainz, FRG, and used as obtained.

polymer films after spin-coating revealed smooth, slightly opaque films. The high volatility of THF caused a radial thickness variation of the films.[16] In all cases the lateral length scales of the thickness variation were much larger than the domain sizes.

Surface Preparation. The substrates used in the experiments were highly polished silicon wafers. Organic residues on the silicon oxide covered surfaces were removed by cleaning the silicon wafer under a jet of CO_2−ice crystals ("snow-jet").[17] The substrates were first covered with a 2 nm thick chrome layer, followed by the evaporation of a 30 nm thick gold (Au) layer. The substrates were used immediately after the deposition of the Au layer. To produce low-energy surfaces, a self-assembled alkane monolayer (SAM) was deposited onto the substrate by immersing Au-covered silicon wafers overnight in a 0.285% solution of octadecylmercaptan in an ethanol−THF mixture (5:2). The resulting surfaces were qualitatively characterized by measuring the static water contact angle. The quality of the SAM layer deteriorates with an increasing organic contamination of the Au surface. Only substrates with a water contact angle of 105° or larger were used.

Atomic Force Microscopy. For topographic imaging, a Park Scientific atomic force microscope (AFM) and a self-built AFM were used. Both microscopes have optical access to the AFM cantilever and tip. All measurements were performed in contact

(16) Kessler, J.; Higashida, N.; Shimomai, K.; Inoue, T.; Ougizawa, T. *Macromolecules* **1994**, *27*, 2448.

(17) Sherman, R.; Hirt, D.; Vane, R. *J. Vac. Sci. Technol.* **1994**, *12*, 1876.

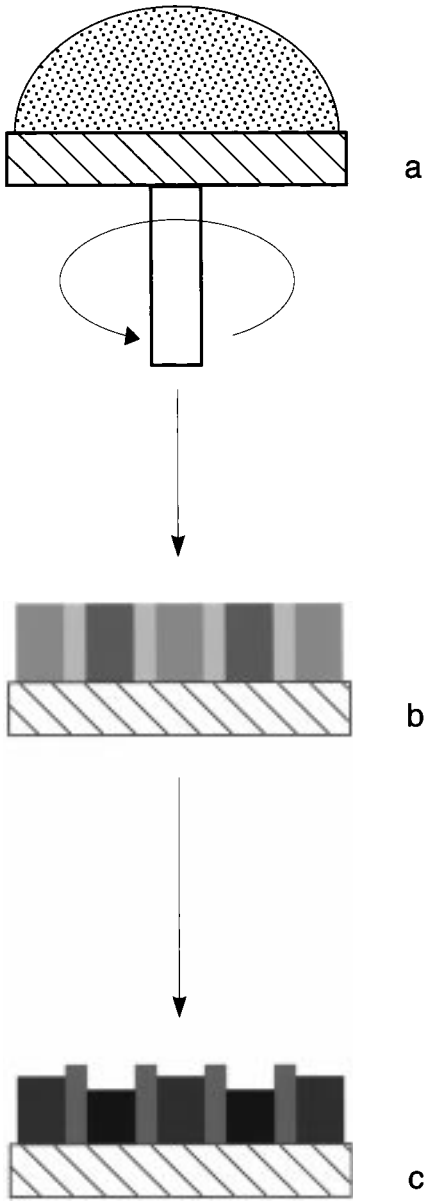

Figure 2. Schematic model describing the formation of the sample topography. Initially, all three polymers and the solvent form one phase (a). During spin-coating, the solvent evaporates and phase separation sets in. At this stage, the film surface is essentially flat (b). Depending on their relative solubility, the three polymer phases contain different solvent concentrations. Due to its poor solubility in THF, the PMMA phase (light gray) solidifies first, followed by a collapse of the PVP (dark gray) and PS (black) phases (c).

mode. To access information on the phase distribution inside the film, the selective solvent technique described by us in an earlier publication[18] was used. First, the sample was marked with several scalpel scratches. AFM scans across such a scratch (not shown here) give information on the overall film thickness. With the help of a stereomicroscope, the AFM tip was positioned next to a characteristic scratch pattern, and a topography image was taken. The sample was then removed from the AFM and washed in ethanol, a selective solvent for PVP, and aligned again with respect to the cantilever tip. A second image of the remaining PS and PMMA phases was taken, scanning the same sample area as in the first image. After the removal of PS by dissolution in cyclohexane, a third topography image was taken again at the same location. The difference of the three images gives information on the phase morphology inside the film. To visualize the polymer distribution normal to the film surface, cross sections taken at identical locations on the three images were superimposed to yield a cross-sectional profile.

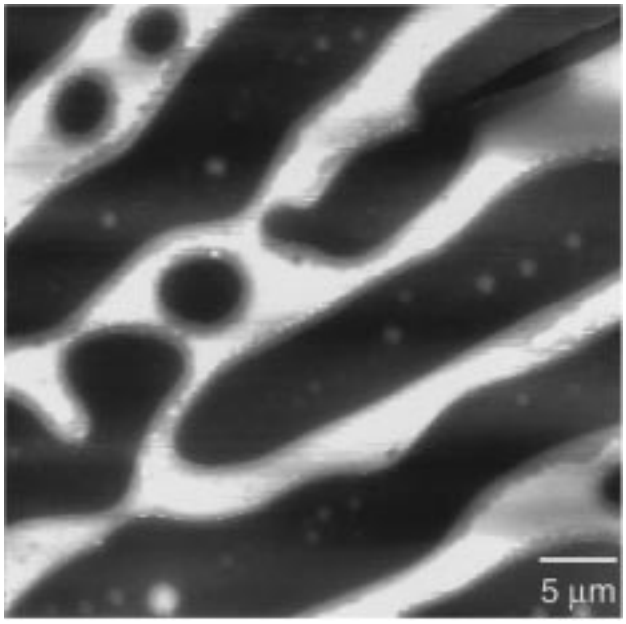

Figure 3. Phase morphology of a PS−PVP mixture (1:1) cast from THF (3% polymer) onto a SAM-covered surface. The characteristic structure sizes (8−10 μm) in the approximately 100 nm thick film are 1 order of magnitude larger compared to the PS−PMMA−PVP system, where the PMMA component acts as an interfacial compatibilizer (Figure 1).

It is important to note that the selective solvent procedure may be prone to artifacts. Insoluble phases embedded in a soluble polymer matrix may be washed away, or thin surface films may not be sufficiently mechanically stable to withstand the washing procedure. However, checks can be employed to rule out any significant contribution of such artifacts.[18]

Results and Discussion

We start our discussion with the domain structures found on a SAM-covered substrate after spin-coating a PS/PMMA/PVP (1:1:1) film from THF (Figure 1a). Using the selective solvent technique, the PVP (Figure 1b) and PS (Figure 1c) phases were removed. The image reveals the lateral phase morphology, which features a PMMA net whose meshes are filled with PS and PVP in an alternating fashion. All three phases extend from the air to the substrate surface. In addition to the lateral domain morphology, the sample exhibits a topographical structure which coincides with the polymer phases. The PMMA net protrudes over the lower lying PS and PVP phases.

First, we turn our attention to the surface topography. As reported by us,[18] the surface corrugation is due to different solubilities of the three polymers in THF. Initially, all three polymers and the solvent form one phase (Figure 2a). During the spin-coating process, the solvent evaporates and coexisting PS-rich, PMMA-rich, and PVP-rich phases form. At this intermediate point, all phases are still liquid due to their solvent content, and the sample surface is essentially flat (Figure 2b). Even though the solvent dissolves all three polymers, the relative solubility of the three polymers in THF varies. THF is a poorer solvent for PMMA than for PS and PVP. Therefore, the PMMA-rich phase contains less THF than the PS and PVP phases. As more solvent evaporates, a characteristic time is passed when there is practically no THF left in the

(18) Walheim, S.; Böltau, M.; Mlynek, J.; Krausch, G.; Steiner, U. *Macromolecules* **1997**, *30*, 4995−5003.

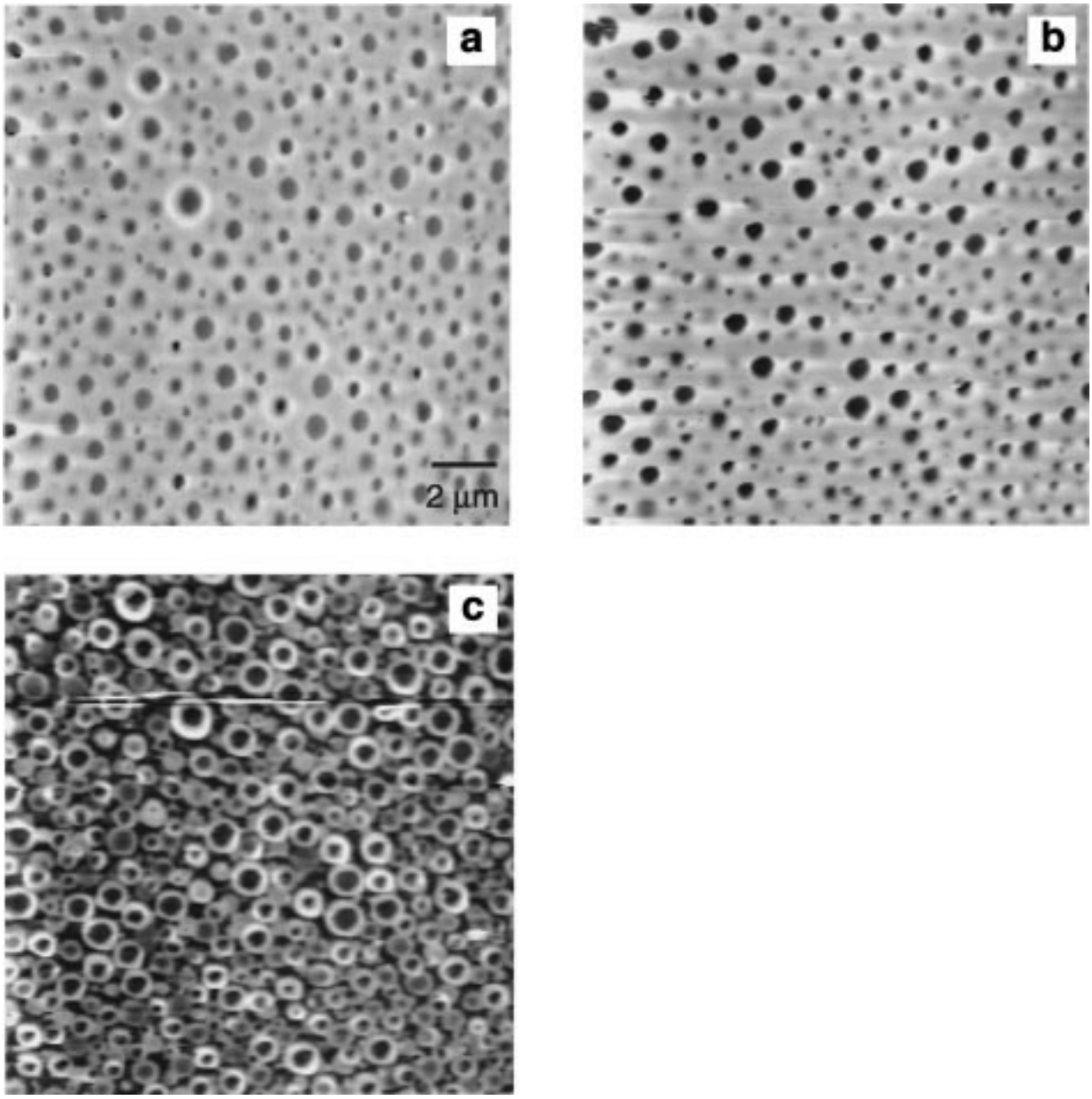

Figure 4. AFM images of a PS/PMMA/PVP film (3:1:1) cast from THF onto a SAM-covered surface: (a) as cast; (b) after immersion in ethanol to remove PVP; (c) after removal of PS by dissolution in cyclohexane. The PVP phase forms circular inclusions in the PS majority phase which are surrounded by PMMA, giving rise to the PMMA rings after removal of the PS and PVP phases (c).

PMMA phase, while the other phases are still swollen with THF. Further evaporation collapses the swollen PS and PVP phases to a level, which lies below the interface of the higher PMMA structures (Figure 2c).

A second aspect is the qualitative description of the PS/PMMA/PVP lateral phase morphology. As is evident from the cross section in Figure 1d, none of the three phases wets or enriches either at the air or at the substrate surface and we can consider the film as a quasi-two-dimensional system. In this case (assuming a Flory−Huggins model), the balance of the three enthalpic interaction parameters governs the phase morphology. For PS, PMMA, and PVP, the PS−PVP interaction parameter ($\chi = 0.1$[19]) is much larger than the values for the PS−PMMA ($\chi \approx 0.02$[20]) and PMMA−PVP ($\chi \approx 0.007$[21]) interfaces. Consequently, the free energy of the PS−PMMA−PVP system can be lowered by minimizing the PS−PVP interfaces. Therefore, the PS−PVP interface is wetted by a PMMA layer which compatibilizes the PS−PVP interface. This is illustrated by the AFM image in Figure 3. Here, the PMMA was omitted and the PS−PVP film, cast from THF, features a mean lateral length scale ($\sim 8\,\mu$m), which is 1 order of magnitude larger compared to the film in Figure 1.

To test whether this astonishingly simple model is useful to describe the phase morphologies of this three-component mixture in general, we varied the volume fractions of the polymers. Three further examples are shown in the Figures 4−6. In a mixture, which contains three times as much PS than PMMA and PVP, we observe circular domains in a PS matrix (Figure 4a). As revealed by the exposure of the sample to ethanol, these domains consist of PVP (Figure 4b). In analogy to Figure 2, the PS−PVP

(19) Shull, K. R.; Kramer, E. J.; Hadziioannou, G.; Tang, W. *Macromolecules* **1990**, *23*, 4780−4787.

(20) Pinder, D. N. *Macromolecules* **1997**, *30*, 226−235.

(21) Unpublished results.

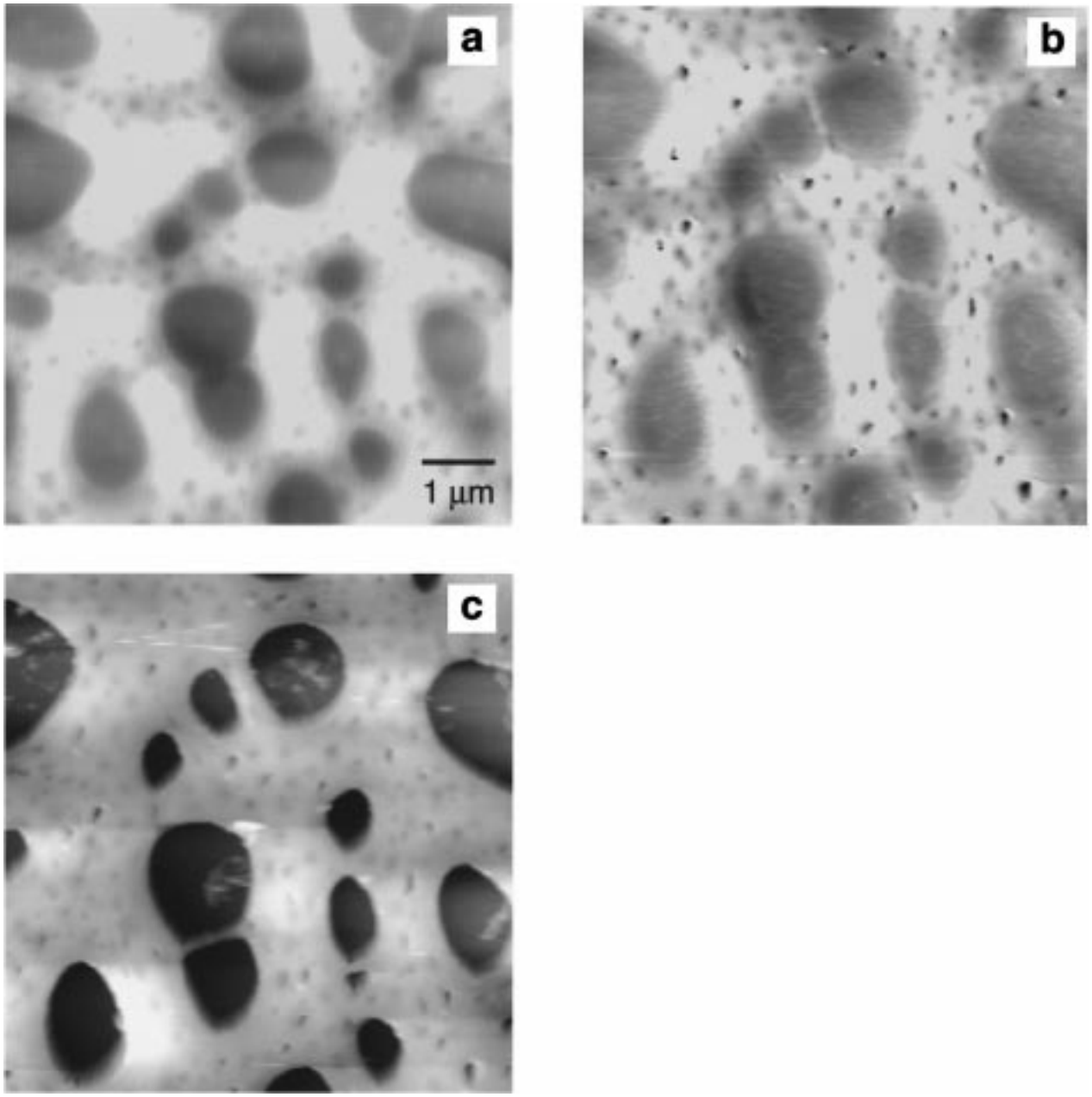

Figure 5. AFM images of a PS/PMMA/PVP film (9:9:2) cast from THF onto a SAM-covered surface: (a) as cast; (b) after immersion in ethanol to remove PVP; (c) after removal of PS by dissolution in cyclohexane. Demixing of the two majority phases (PS and PMMA) leads to a length scale of ~1 μm. In addition, the continuous PMMA phase exhibits small PVP inclusions with a diameter of ~100 nm.

interface is wetted by the PMMA phase. Once the PS matrix is removed by dissolution in cyclohexane (Figure 4c), doughnut-like PMMA rings appear on the unpolar substrate.

Another sample contained less PVP compared to PS and PMMA (9:9:2 PS/PMMA/PVP). In Figure 5, we observe two lateral length scales. The demixing of PMMA and PVP gives rise to a coarse mesh (structure size ~ 1 μm) (Figure 5a), revealed by dissolution of the PS phase in cyclohexane (Figure 5c). The remaining PMMA ridges are pock-marked by the minority phase: small PVP inclusions with a mean diameter of ~100 nm (Figure 5b,c).

To test the robustness of the principle described above, we reduce the relative amount of PMMA (2:1:2 PS/PMMA/PVP) (Figure 6a). The film reveals that the emulsifying function of the PMMA component is partially lost and two length scales are observed: a coarse bicontinuous phase morphology with a characteristic periodicity of ~7 μm and small inclusions with a diameter of $\leq$0.5 μm. Dissolution in ethanol (Figure 6b) and cyclohexane (Figure 6c) reveal that, also in this case, a thin PMMA layer intercalates at the PS−PVP interface. Remarkably, the width of these thin PMMA stripes is in the order of the film thickness (~100 nm).

The choice of the substrate surface is absolutely instrumental for our model experiment. In Figure 7, the unpolar SAM surface has been replaced by a polar silicon oxide (SiO_x) substrate. At first sight, a film cast from the same solution as in Figure 1 seems to feature a similar topography as on the SAM surface (Figure 7a). However, placing the sample for a brief period of time into ethanol does not change the sample topography. If the sample is exposed to ethanol for several minutes, the entire film floats off the substrate. This observation strongly suggests that PVP is not present at the air surface but covers the SiO_x substrate. To test this assumption, we first remove

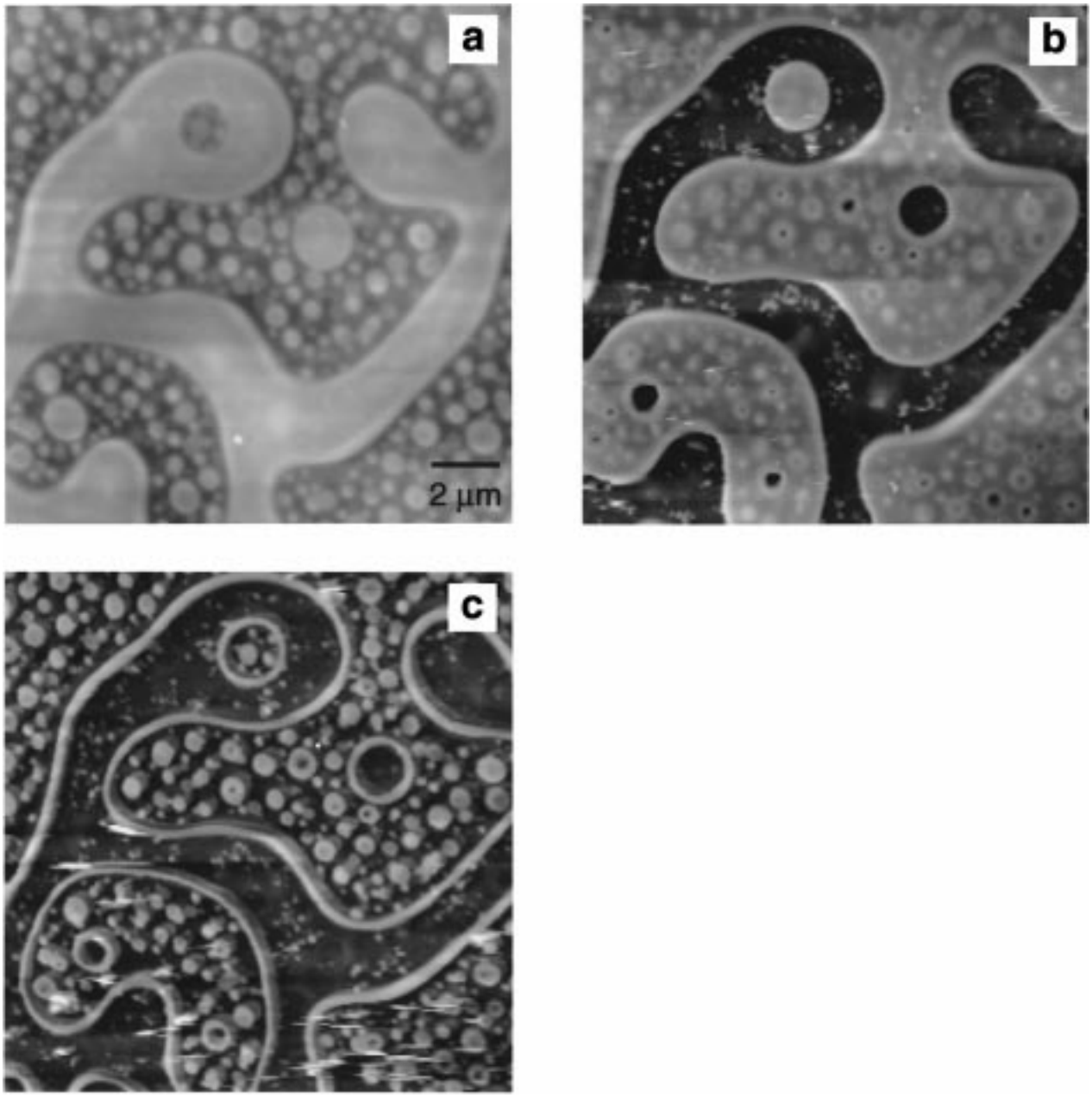

Figure 6. AFM images of a PS/PMMA/PVP film (2:1:2) cast from THF onto a SAM-covered surface: (a) as cast; (b) after immersion in ethanol to remove PVP; (c) after removal of PS by dissolution in cyclohexane. Due to a reduction in PMMA volume fraction, the compatibilizing effect is partially lost. The patterns on a 8 μm length scale are reminiscent of the PS−PVP blend from Figure 3; the smaller domain sizes (1 μm) are similar to Figure 1.

the PS by dissolution in cyclohexane (Figure 7b). Again, a brief immersion of the sample in ethanol does not change the sample topography. The next step, the selective dissolution of the PMMA phase, is not trivial since we did not find a solvent that only dissolves PMMA and leaves the PVP untouched. Xylol, however, is a good solvent for PMMA and a poor solvent for PVP. By briefly (1 min) immersing the sample in xylol, the PMMA phase is completely removed, while very little of the PVP is dissolved. In Figure 7c, a homogeneous PVP layer is revealed. The layer exhibits a surface undulation, which is correlated with the PS−PMMA phase morphology in Figure 7a.

This result can be compared to an earlier study on the demixing of PS and PMMA on polar and unpolar substrates.[18] In Figure 8, a PS−PMMA mixture which was spin-cast from THF onto a SiO_x surface reveals a similar phase morphology compared to Figure 7. This comparison gives some insight into the formation of the phase morphology in Figure 7. During spin-coating, the PVP forms a complete wetting layer on the SiO_x surface. On top of this layer, lateral demixing of PS and PMMA is observed in a similar fashion as in Figure 8. It is important to note that the PS domains in Figure 7 are separated by a thin PMMA film from the PVP wetting layer which is caused by the strong PS−PVP incompatibility.

The results from Figures 1−6 closely resemble numerical studies by Nauman et al.[6] In their study, Nauman and co-workers consider a ternary liquid in a two-dimensional geometry. As a function of the relative strength of the three interaction parameters and the relative mixing ratios, they obtain images, some of which bear a striking resemblance to our experiments. In Figure 9, we show a reproduction of four images from ref 6[22] in

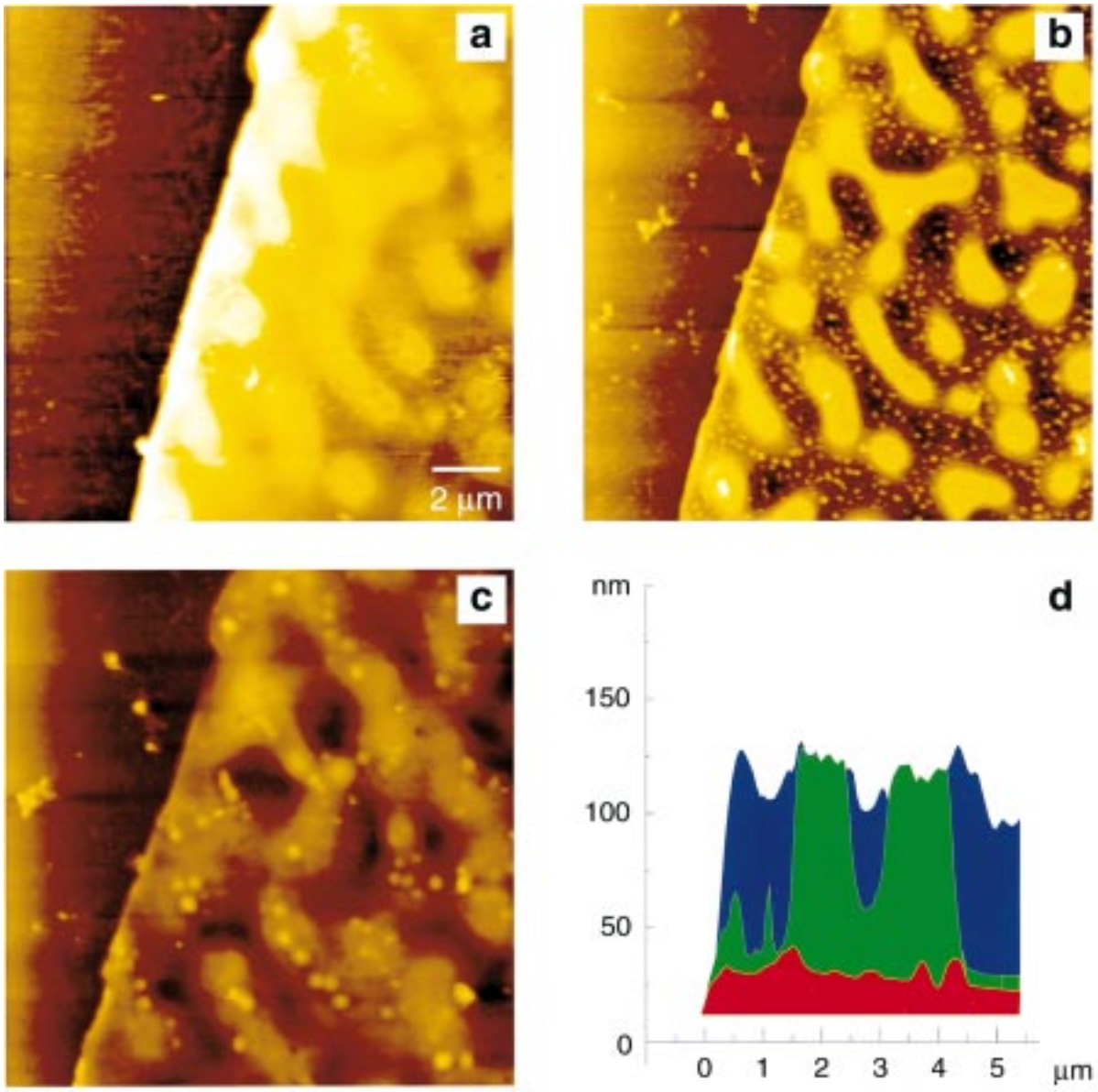

Figure 7. AFM images of a PS/PMMA/PVP film (1:1:1) cast from THF onto a SiO_x surface: (a) as cast; (b) after removal of PS by dissolution in cyclohexane; (c) after removal of PMMA by dissolution in xylol. The superposition of cross sections from (a) to (c) show that the polar substrate is covered by a homogeneous PVP layer (red), which is covered by a laterally demixed phase morphology of PS (blue) and PMMA (green).

which the simulation parameters correspond to the experimental situations of Figures 1, 4, 5, and 6. While parts a and b of Figure 9 exhibit good agreement with the experimental realizations, parts c and d of Figure 9 show only some qualitative similarities. As in Figure 5, the minority phase in Figure 9c forms inclusions in the continuous phase, but these inclusions are fewer and bigger. In Figure 9d, the minority phase wets the interface between the two more incompatible phases, but neither the loss of compatibilization nor the second, smaller length scale of Figure 6 is observed. These discrepancies may be due to a difference in the ratios of the interaction parameters. In the simulations the interaction parameter of the high-energy interface was the sum of the other two interaction parameters. In our experiments, χ(PS−PVP) is approximately four times higher compared to χ(PS−PMMA) + χ(PMMA−PVP).

(22) The figures from the original publication[6] were converted to gray scale.

Conclusions

We present experimental results on the phase morphology of three-component polymer mixtures spin-cast onto unpolar substrates. Despite the complexity of the experimental system and a preparation method, in which the polymer demixing takes place during the rapid evaporation of a solvent, the phase separation process seems to be governed by a single, simple principle. If, as in our system, one of the polymer−polymer interaction parameters exceeds the sum of the other two, the overall free energy can be lowered, if the systems avoids the formation of such interfaces. In this case, the third component intercalates at this interface and forms a wetting layer. The results of the experiments, in which the mixing ratios of the three polymers were systematically varied, are consistent with this model. In addition, numerical simulations by Nauman et al. based on the same model reveal practically identical phase morphologies.

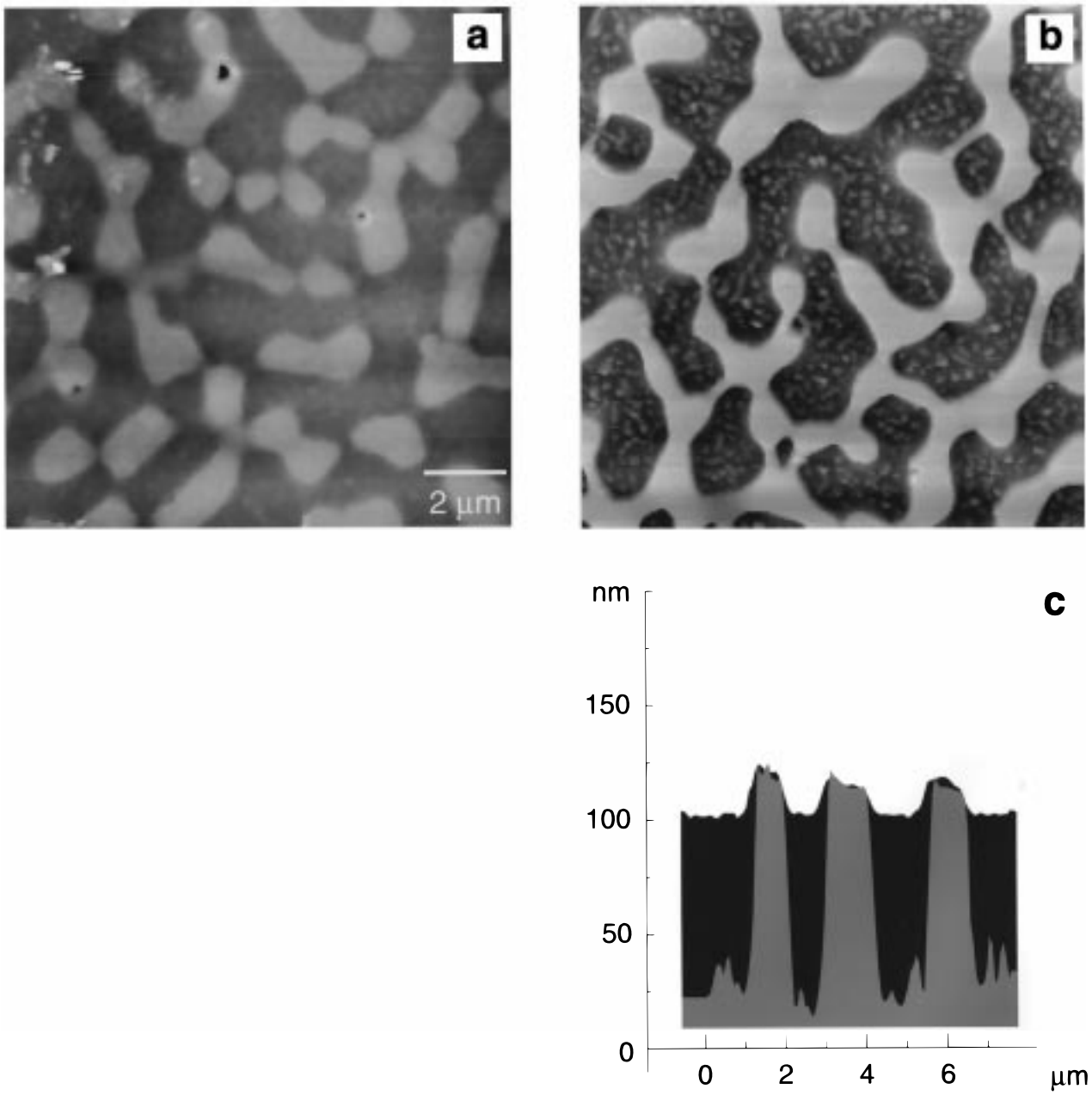

Figure 8. Phase morphology of a PS−PMMA mixture (1:1) cast from THF onto a SiO_x surface (adapted from ref 18): (a) as cast; (b) after removal of PS by dissolution in cyclohexane; (c) superposition of cross sections from (a, b) (PS, black; PMMA, light gray). The characteristic PS−PMMA phase morphology is very similar to that shown in Figure 7. This suggests that the PVP layer in Figure 7 forms first, followed by a phase separation process of PS and PMMA, which is analogous to the demixing of a PS−PMMA blend.

While the explanation of the phase morphology seems strikingly simple, its formation process is not clear. Detailed studies on the demixing process during spin-coating are necessary to confirm our model, which is based on equilibrium arguments. Also, it is important to note that the spin-coating procedure corresponds to a rapid quench caused by the evaporation of the solvent. Therefore, the phase morphologies described here may be far from thermodynamic equilibrium. An annealing experiment to equilibrate the films is, however, not possible for the systems presented here. This is due to the lack of thermal stability of the SAM layer. Future experiments using silane-based SAMs will allow equilibration experiments, which will yield insight into this question.

Our results suggest an application of the demixing of three-component blends for nanolithography. In analogy to earlier work,[23] it is possible to orient the polymer phase morphology on a prestructured substrate.[24] By reducing the volume fraction of the intercalating phase, it should be possible to achieve lateral structures in polymer films which lie much below 1 μm and which feature high aspect ratios.

Acknowledgment. We thank J. Mlynek for his support, E. Neumann for her help with some of the experiments, D. Q. He for supplying Figure 9, and E. Schäffer for his help with the manuscript. This work was supported by the Deutsche Forschungsgemeinschaft

(23) Böltau, M.; Walheim, S.; Mlynek, J.; Krausch, G.; Steiner, U. *Nature* **1998**, *391*, 877−879.
(24) Walheim, S.; Steiner, U. In preparation.

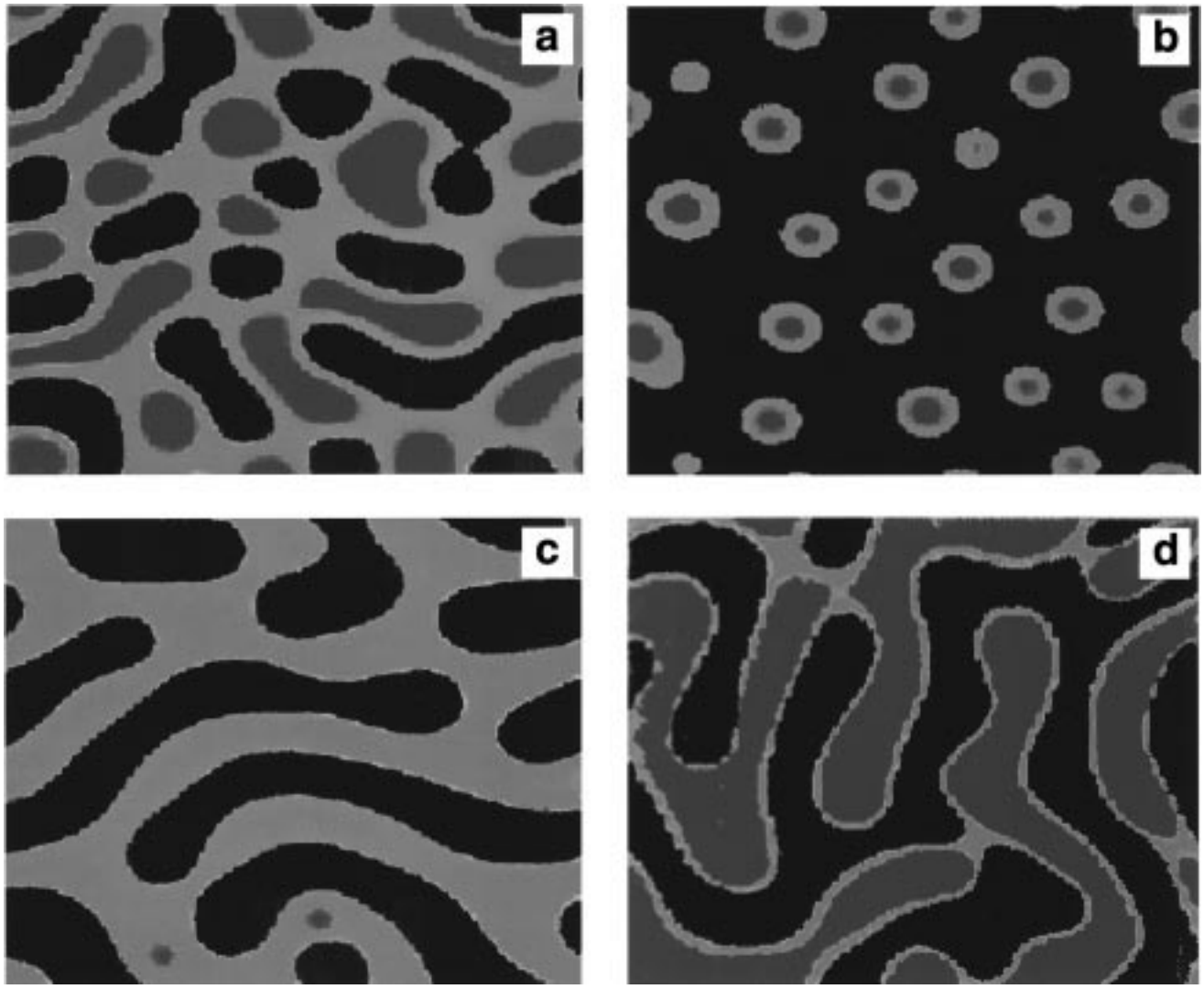

Figure 9. Simulation results by Nauman et al.[6] for ternary polymer mixtures. In all four images, one of the mutual interaction parameters was twice as high as the other two. The phase morphologies (PS, black; PVP, dark gray; PMMA, light gray[22]) in (a) for a 1:1:1 mixture and in (b) for a 3:1:1 mixture show a striking resemblance to Figures 1 and 4, respectively. Predictions for the 9:9:2 (c) and 2:1:2 (d) mixtures, however, only qualitatively resemble the experimental situation in Figures 5 and 6. Reprinted with permission from ref 6. Copyright 1994 Elsevier.

(DFG) (Sonderforschungsbereich 513 B2; Schwerpunkt "Benetzung und Strukturbildung and Grenzflächen"). U.S. acknowledges financial support by a research fellowship (Habilitations-Stipendium) of the DFG.

Supporting Information Available: Color images of Figures 2−6, 8, and 9. This material is available free of charge via the Internet at http://pubs.acs.org.

LA981467E